

Proceedings of the Korean Nuclear Spring Meeting
Gyeong ju, Korea, May 2003

A Numerical Analysis on Thermal Stratification Phenomenon in the SCS Piping

Kwang Chu Kim, Man Heung Park and Hag Ki Youm
Sun Ki Lee* and Tae Ryong Kim*

Korea Power Engineering Company, Inc.
360-9, Mabuk-Ri, Kusong-Eup
Yongin-Shi, Korea 449-713

* Korea Electric Power Research Institute
Taejon-Shi, Korea 305-380

Abstract

A numerical study is performed to estimate on an unsteady thermal stratification phenomenon in the Shutdown Cooling System(SCS) piping branched off the Reactor Coolant System(RCS) piping of Nuclear Power Plant.

In the results, turbulent penetration reaches to the 1st isolation valve. At 500sec, the maximum temperature difference between top and bottom inner wall in piping is observed at the starting point of horizontal piping passing elbow. The temperature of coolant in the rear side of the 1st isolation valve disk is very slowly increased and the inflection point in temperature difference curve for time is observed at 2700sec. At the beginning of turbulent penetration from RCS piping, the fast inflow generates the higher temperature for the inner wall than the outer wall in the SCS piping. In the case the hot-leg injection piping and the drain piping are connected to the SCS piping, the effect of thermal stratification in the SCS piping is decreased due to an increase of heat loss compared with no connection case. The hot-leg injection piping affected by turbulent penetration from the SCS piping has a severe temperature difference that exceeds criterion temperature stated in reference. But the drain piping located in the rear compared with the hot-leg injection piping shows a tiny temperature difference.

In a viewpoint of designer, for the purpose of decreasing the thermal stratification effect, it is necessary to increase the length of vertical piping in the SCS piping, and to move the position of the hot-leg injection piping backward.

1. Introduction

The thermal stratification phenomenon is that flow is stabilized with temperature layers due to the density difference between hot and cold water. This thermal stratification in piping

is capable of causing the bending stress, a serious deformation in piping, and the support damage. Specially, the periodic thermal stratification is capable of causing the thermal fatigue cracking of piping[1].

It has been reported that thermal stratification phenomena in nuclear power plant(NPP) are mainly observed in surge line of pressurizer, feedwater system line, safety injection system line, residual heat removal system line, and chemical and volume control system line during the transient(startup or hot standby) or normal operating conditions[2-5]. USNRC Bulletin 88-08 demands to evaluate the main piping in NPP expected to occur the thermal stratification using analytic evaluation, design improvement or ultrasonic testing[3]. In Korea, the regulation and the inspection for the piping branched off Reactor Coolant System(RCS) piping have been intensified, and the study for these piping has been actively carried out[6-10].

In this study, an unsteady analysis on thermal stratification in the Shutdown Cooling System(SCS) piping branched off the RCS piping is carried out. With the results of analysis, the method for minimizing the thermal stratification effect is tried to find.

2. Model Description

2.1 Analysis Scope

The schematic diagram for SCS piping connected to RCS piping is showed in Fig.1.

The SCS of nuclear power plant takes charge of function to remove continually heat when the reactor shutdown occurs. The SCS called in CE type plants is functionally identical with the Residual Heat Removal System(RHRS) called in Westinghouse type plants. Korea Standard Nuclear Power Plant(KSNP) concerned in this study is included in CE type plants.

All valves in the SCS piping are isolated during normal or startup operating condition. Also, turbulent penetration that the higher temperature coolant out of the RCS piping penetrates into the SCS piping that is stagnant occurs. In the Fig.1, the RCS hot-leg that the higher temperature coolant passes is piping that the inner diameter is 1.07m(42"). The SCS piping concerned in this study is piping that the nominal diameter is 0.406m(16") and SCH. is 160. Also, the SCS piping has the hot-leg injection piping and the drain piping. The nominal diameter of the hot-leg injection piping is 0.076m(3") and the nominal diameter of the drain piping is 0.051m(2").

2.2 Governing Equations

Unsteady, incompressible and three dimensional conservation equations are used as governing equation for the thermal flow analysis. The standard k- ϵ model is used for turbulent model and the Boussinesq's approximation is used for the buoyancy effects. Assuming that all properties are constant under given temperature and pressure, the used governing equations are as follows;

$$\frac{\partial}{\partial x_i}(\mathbf{r}u_i) = 0 \quad (1)$$

$$\frac{\partial}{\partial t}(\mathbf{r}u_i) + \frac{\partial}{\partial x_j}(\mathbf{r}u_j u_i) = -\frac{\partial p}{\partial x_i} + \mathbf{r}g_i \mathbf{b}(T - T_{cold}) + \frac{\partial}{\partial x_j} \left[(\mathbf{m} + \mathbf{m}_i) \left(\frac{\partial u_i}{\partial x_j} + \frac{\partial u_j}{\partial x_i} \right) - \frac{2}{3} k \mathbf{d}_{ij} \right] \quad (2)$$

$$\frac{\partial}{\partial t}(\mathbf{r}T) + \frac{\partial}{\partial x_j}(\mathbf{r}u_j T) = \frac{\partial}{\partial x_j} \left\{ \left(\frac{\mathbf{m}}{\text{Pr}} + \frac{\mathbf{m}_i}{\mathbf{s}_i} \right) \frac{\partial T}{\partial x_j} \right\} \quad (3)$$

$$\frac{\partial}{\partial t}(\mathbf{r}k) + \frac{\partial}{\partial x_j}(\mathbf{r}u_j k) = \frac{\partial}{\partial x_j} \left[\left(\mathbf{m} + \frac{\mathbf{m}_i}{\mathbf{s}_k} \right) \frac{\partial k}{\partial x_j} \right] + P_k + G_b - \mathbf{r}e \quad (4)$$

$$\frac{\partial}{\partial t}(\mathbf{r}e) + \frac{\partial}{\partial x_j}(\mathbf{r}u_j e) = \frac{\partial}{\partial x_j} \left[\left(\mathbf{m} + \frac{\mathbf{m}_i}{\mathbf{s}_e} \right) \frac{\partial e}{\partial x_j} \right] + \frac{e}{k} [C_1(P_k + G_b) - C_2 \mathbf{r}e] \quad (5)$$

where, the coefficient, source term and turbulent constants used in governing equations are as follows;

$$\mathbf{m}_i = \mathbf{r}C_m \frac{k^2}{e}$$

$$P_k = \mathbf{m}_i \left(\frac{\partial u_i}{\partial x_j} + \frac{\partial u_j}{\partial x_i} \right) \frac{\partial u_i}{\partial x_j}$$

$$G_b = -\frac{\mathbf{m}_i}{\mathbf{s}_i} g_i \mathbf{b} \frac{\partial T}{\partial x_i}$$

$$\mathbf{s}_i = 0.85, \mathbf{s}_k = 1.0, \mathbf{s}_e = 1.3, C_m = 0.09$$

$$C_1 = 1.44, C_2 = 1.92$$

2.3 Boundary Conditions

Temperature and flow rate of coolant in inlet of the hot-leg are 600K and 7718kg/s respectively, and turbulent intensity of 10% for hydraulic diameter is assumed. The outlet boundary condition is the constant pressure condition. All outer surfaces of piping including the hot-leg are assumed to be adiabatic wall. All valves in the SCS piping, the hot-leg injection piping and the drain piping are assumed to be isolated. There is no leakage throughout disk. The disk thickness in valve is assumed to be as two times as piping thickness. Each end surface of branch piping in the range of analysis is assumed to be

isolated and to be a low temperature wall of 322K. In the process of the numerical calculation, initial temperature condition is set to be 322K. The values for condition of average temperature in 15.5MPa are used for the properties of fluid. The material of solid is assumed to be SUS304.

2.4 Numerical Analysis

The Fluent 5.5 code is used for analysis on thermal stratification in the SCS piping. The grid system is shown in Fig. 2. The number of cells is 87,776. The length from the connection point of the hot-leg with the SCS piping to the outlet of the hot-leg is assumed to be more than 20 times of the SCS piping diameter to reflect on flow change in connection part and to improve convergence. The range of analysis for the SCS piping, the hot-leg injection piping, and the drain piping is set to the extend of suitable length passing the 1st valve in consideration of thermal stratification effect and support position.

The SIMPLE algorithm is used to calculate the pressure field at each cell. The first order upwind scheme is used to determine the convection term. The convergence criterion is that residual is less than 1.0×10^{-5} for continuity and 1.0×10^{-7} for momentum, energy and turbulent at the each time step. To satisfy this convergence criterion, iteration less than 50 times per time step of 1 second are needed. To improve the convergence, the under-relaxation factors on pressure, temperature, velocity, and turbulent terms are applied.

3. Results and Discussions

Fig. 3 to Fig. 6 shows the temperature distributions for various times in the SCS piping including the hot-leg injection piping and the drain piping.

Fig. 3 shows the result of temperature distribution at 100sec. The vertical part in the SCS piping shows rapid turbulent penetration from the RCS hot-leg. Also, thermal stratification effect due to turbulent penetration from the SCS piping appears in the horizontal part of the hot-leg injection piping. At the beginning, the fast inflow from the RCS piping generates the higher temperature for the inner wall than the outer wall in the SCS piping.

Fig. 4 shows the temperature distribution at 500sec. Thermal stratification phenomenon is shown in the horizontal part of the SCS piping. However, thermal stratification effect in the hot-leg injection piping was largely decreased despite of continuous temperature penetration. This can be judged to result from a strong thermal mixing effect as the piping diameter is small.

Fig. 5 shows the temperature distribution at 800sec. The temperature difference between inner wall and outer wall is a little bit. In addition, top-to-bottom temperature difference in horizontal piping of the SCS piping is decreased considerably. In the course of unsteady state, the drain piping did not show the outstanding effect of thermal stratification. This result can be judged to be because the thermal mixing effect is big due to the small diameter of the drain piping, the horizontal part is short, and turbulent penetration intensity is decreased as piping is located backward considerably.

Fig. 6 shows the temperature distribution at 2500sec. Top to bottom stratification gradient in all piping disappeared. The surface between the front and the rear of 1st valve disk showed

a severe temperature gradient and the temperature of coolant in rear side was increased slightly. This result is judged to be due to conduction heat transfer in the disk and low temperature coolant that heat capacity is larger than solid.

Fig. 7 shows the schematic diagram for the positions of temperature measurement. In all, nine positions were investigated for the SCS piping, the hot-leg injection piping, and the drain piping.

Fig. 8 represents the temperature changes for the variations of time at the point 1 in vertical part of the SCS piping that is near the hot-leg. Four points that were located at interval of 90° in cross-sectional area were examined. At the beginning of turbulent penetration from the hot-leg, each point has the different temperature due to the flow direction in hot-leg and the difference of penetration intensity at each point. Thus, the temperature difference between I and III point is higher than that between II and IV. However, the temperature difference is decreased as time passes, and the temperature values at all points begin to be similar after 400 sec.

Fig. 9 shows the temperature changes for the variations of time at the point 2. Due to the continuous turbulent penetration, initially rapid temperature increment appears, but there is very small temperature difference among points in all times.

Fig. 10 shows the temperature difference changes between top and bottom inner wall at the point 3 and 4 for the variations of time. The point 3 is located in the starting point of the horizontal part passing the 1st elbow. The maximum temperature difference of 35°F is observed at 500sec. However, the temperature difference is decreased after 500sec. The point 4 is the rear side of the 1st valve disk. The temperature of coolant in the rear side of the 1st isolation valve disk is very slowly increased and the inflection point in temperature difference curve for time is observed at 2700sec. The maximum temperature difference is about 27°F. This result represents that the thermal stratification effect of coolant in rear side of the 1st isolation valve, unless the valve has the leakage, is not significant.

Fig. 11 represents the temperature difference changes between top and bottom inner wall at the point 5, 6 and 7 for the variations of time. The point 5 to 7 is located in the horizontal part of the hot-leg injection piping connected with the SCS piping. As all points are directly affected by turbulent penetration from the SCS piping, a severe temperature difference appears and exceeds the criterion temperature(50°F) stated in reference[1,3,11].

Fig. 12 represents the temperature difference changes between top and bottom inner wall at the point 8 and 9 for the variations of time. These points are located in the horizontal part of the drain piping connected with the SCS piping. The temperature difference appears but is tiny. It is judged that this result is because the drain piping is located backward compared with the hot-leg injection piping and the magnitude of turbulent penetration from the SCS piping is a bit.

Fig. 13 shows the temperature difference changes between top and bottom inner wall at the point 3 and 4 for the variations of time in the case that the hot-leg injection piping and the drain piping are not connected with the SCS piping. The temperature change shape is similar with Fig. 10, but the maximum temperature difference shows an increase of 1.5 times compared with the case without the hot-leg injection piping and the drain piping. This result shows that no heat loss to the hot-leg injection piping increases the effect of the thermal stratification of the SCS piping.

4. Conclusion

A numerical study was performed to estimate on an unsteady thermal stratification phenomenon in the SCS piping branched off the RCS piping in NPP. At 500sec, the maximum temperature difference between top and bottom inner wall in piping is observed at the starting point of horizontal part passing elbow. The thermal stratification effect of coolant in rear side of the 1st isolation valve, unless valve has the leakage, is not significant.

To decrease the thermal stratification in the horizontal piping of the SCS piping, the vertical piping layout connected with the RCS piping is significant. In the vertical piping, if heat loss is increased and turbulent penetration intensity is decreased, the thermal stratification effect in the horizontal piping can be decreased. To achieve this purpose, the length of the vertical piping needs to be increased.

In the case the hot-leg injection piping is connected with the vertical piping of the SCS piping, the thermal stratification effect in the horizontal piping of the SCS piping is decreased due to heat loss and flow loss to the hot-leg injection piping. On the other hand, the thermal stratification effect in the hot-leg injection piping is showed largely and thermal stratification effect in the drain line is tiny. This is because hot-leg injection piping is more influenced by turbulent penetration intensity than drain piping located backward compared with the hot-leg injection piping. Thus, in order to decrease the thermal stratification effect in hot-leg injection piping, it is necessary to move the position of the hot-leg injection piping to the rear that the influence of turbulent penetration intensity from the RCS piping is less reached as possible.

References

1. EPRI, "Thermal Stratification, Cycling and Striping(TASCS)", TR-103581, 1994.
2. "Nuclear Power Experience(NPE)", Published by RCG/Hagler, Bailly, Inc., Boulder, Co., 1993.
3. NRC, "Thermal Stresses in Piping Connected to Reactor Coolant Systems", Bulletin No. 88-08, 1998.
4. NRC, "Cracking in Feedwater System Piping", Bulletin No. 79-13, 1979.
5. NRC, "Pressurizer Surge Line Thermal Stratification", Bulletin No. 88-11, 1988.
6. Man-Heung Park, et al, "Numerical Analysis on the Natural Convection in a Long Horizontal Pipe with Thermal Stratification", 14th UIT National Heat Transfer Conference, 1996.
7. Hagki Youm, et al, "Numerical Analysis for Unsteady Thermal Stratified Turbulent Flow in a Horizontal Circular Cylinder", ICONE-4 Conference, 1996.
8. KEPRI & KOPEC, "Pressurized Thermal Shock Evaluation for Reactor Pressure Vessel of Kori Unit 1", Technical Report-TR.96BJ12.J1999.81, 1999.
9. Hagki Youm, et al, "Development of Numerical Analysis Model for Thermal Mixing in the Reactor Pressure Vessel", ASME, PVP-2000 Conference, 2000.
10. Man-Heung Park, et al, "Numerical Study on Thermal Mixing Flow in Cold Leg during Loss of Coolant Accident", ASME, PVP-2001 Conference, 2001
11. CEOG Owners Group, "Summary of Programs in Response to NRC Bulletin 88-08(CEOG Task 866)", CE NPSD-1043, 1996.

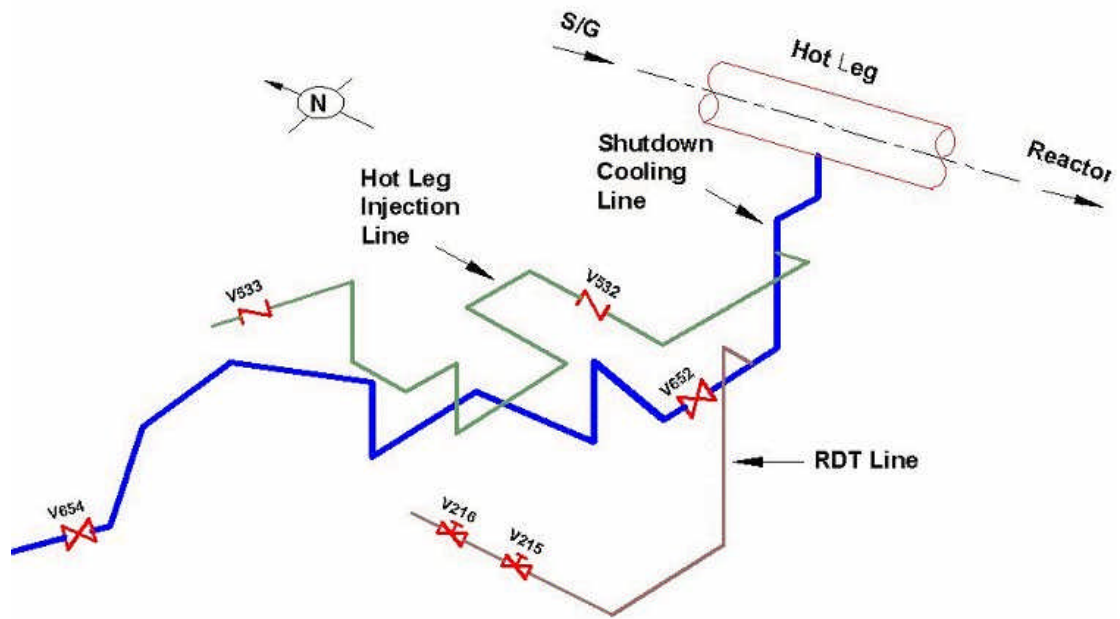


Fig. 1 Schematic diagram for the SCS piping connected to the RCS piping

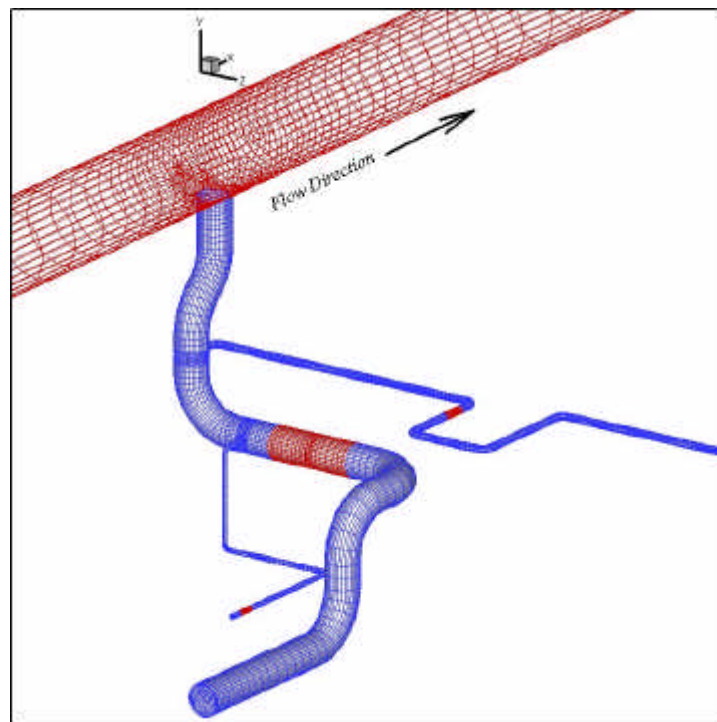
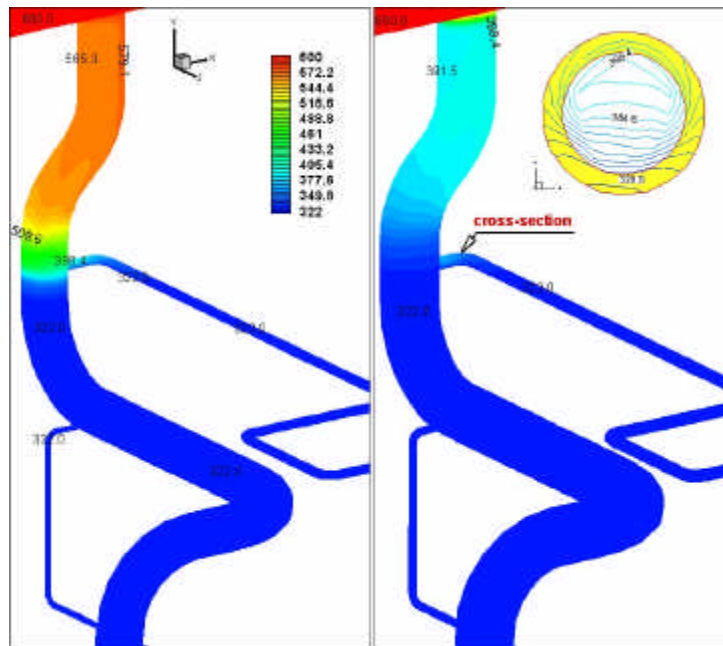


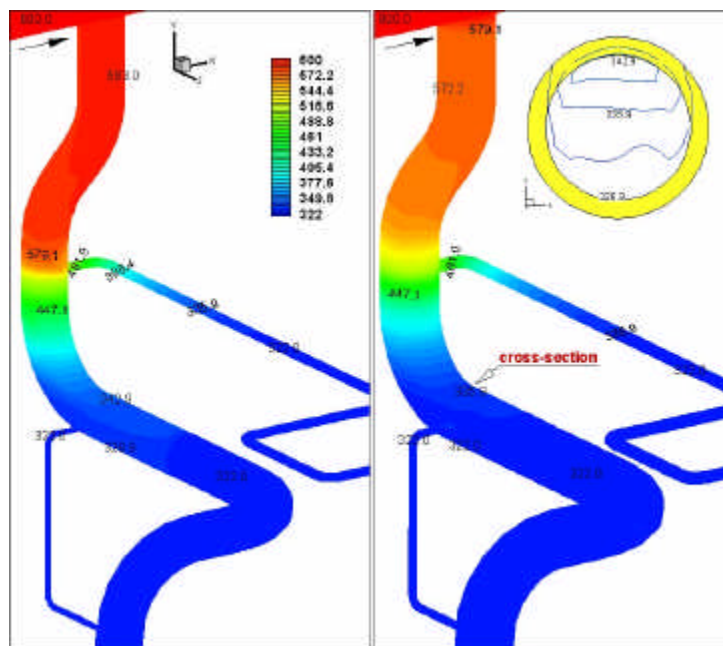
Fig. 2 Grid System for the SCS piping including the RCS piping



(a) inner wall

(b) outer wall

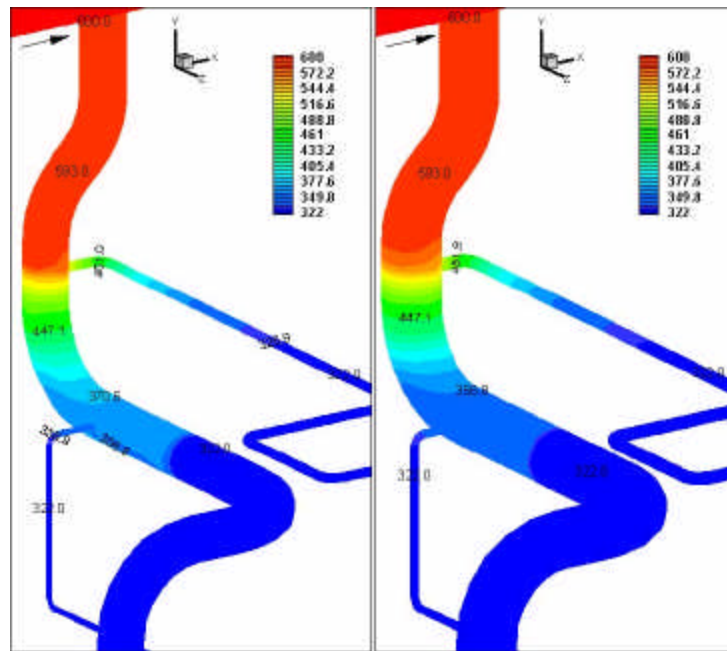
Fig. 3 Temperature distributions for various times in the SCS piping (t=100sec)



(a) inner wall

(b) outer wall

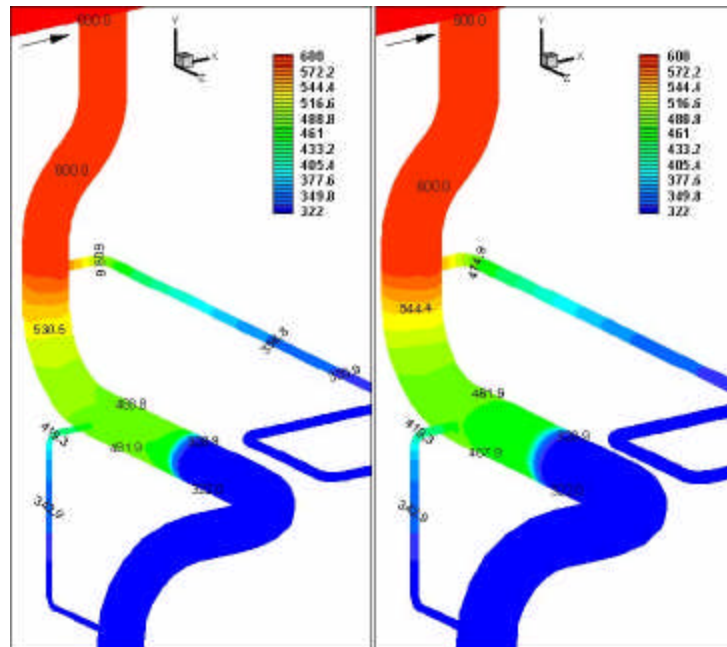
Fig. 4 Temperature distributions for various times in the SCS piping (t=500sec)



(a) inner wall

(b) outer wall

Fig. 5 Temperature distributions for various times in the SCS piping (t=800sec)



(a) inner wall

(b) outer wall

Fig. 6 Temperature distributions for various times in the SCS piping (t=2500sec)

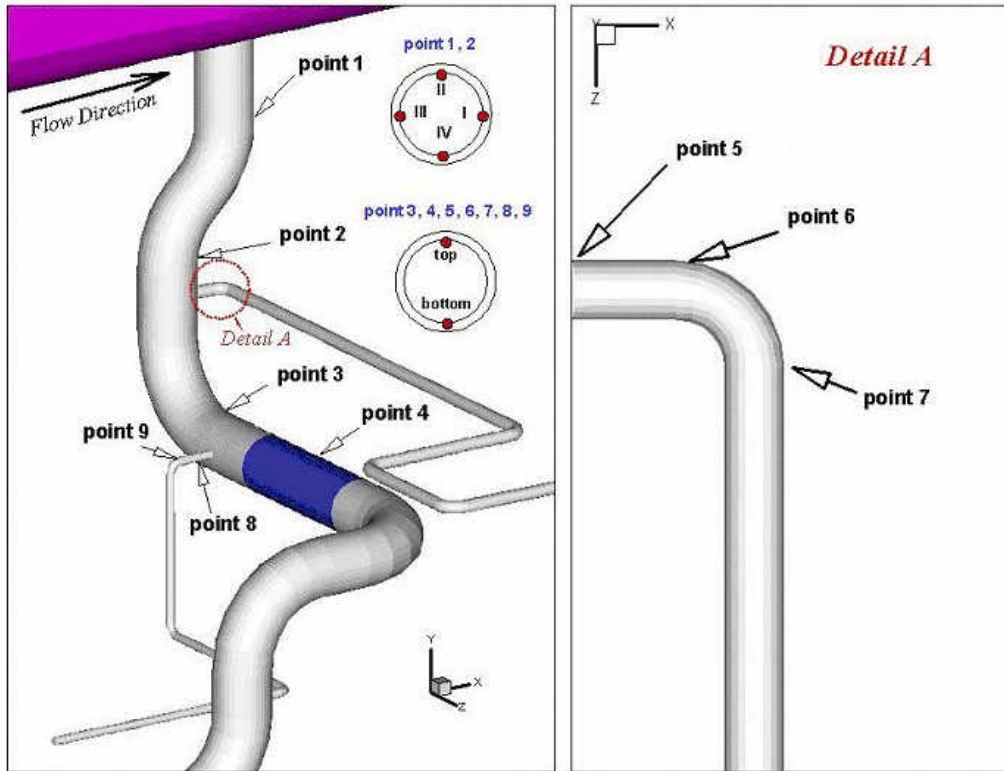


Fig. 7 Schematic diagram for the positions of temperature measurement

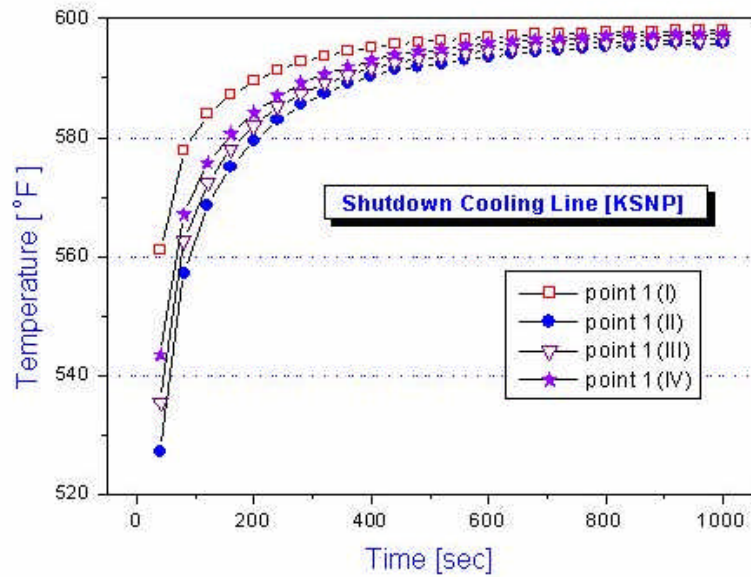


Fig. 8 Temperature changes for the variations of time at the point 1

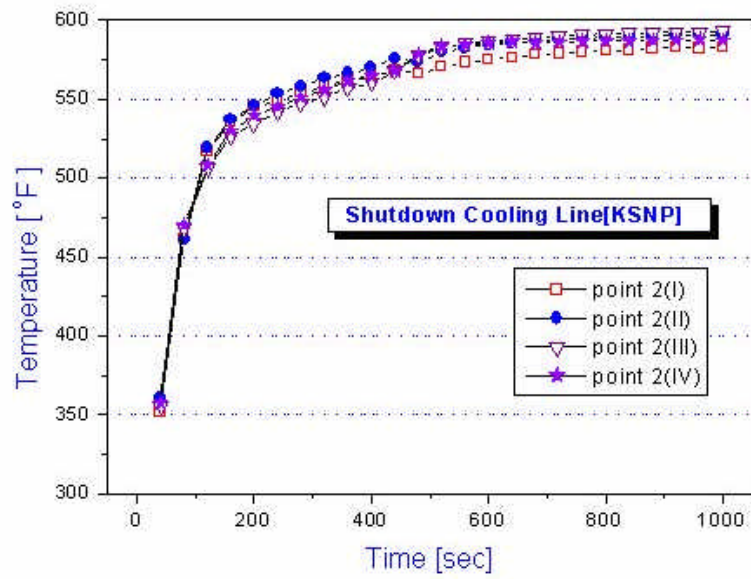


Fig. 9 Temperature changes for the variations of time at the point 2

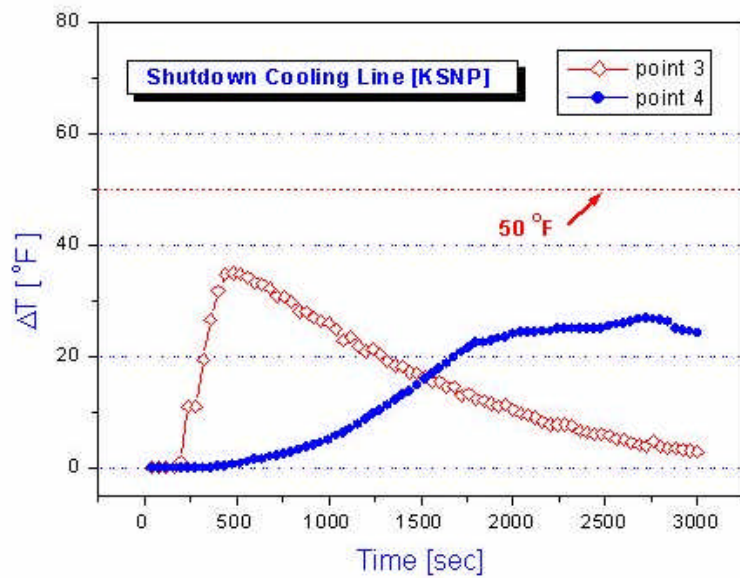


Fig. 10 The temperature difference changes between top and bottom inner wall at the point 3 and 4 for the variations of time

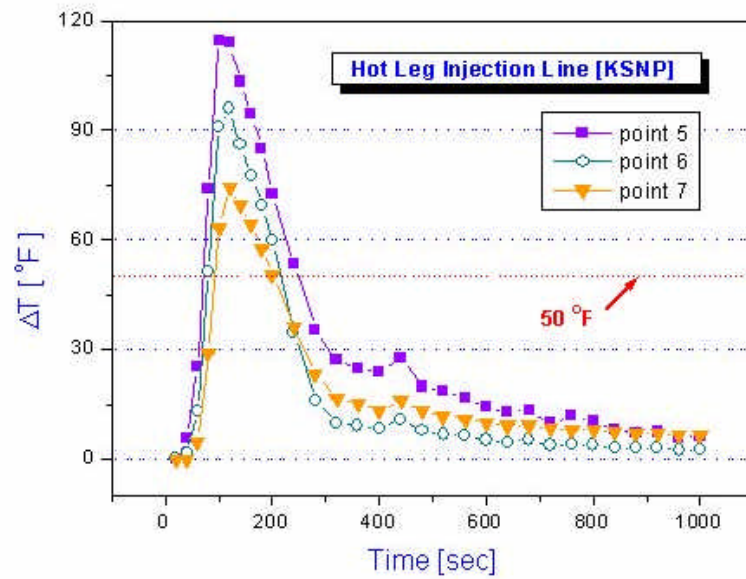


Fig. 11 The temperature difference changes between top and bottom inner wall at the point 5, 6 and 7 for the variations of time

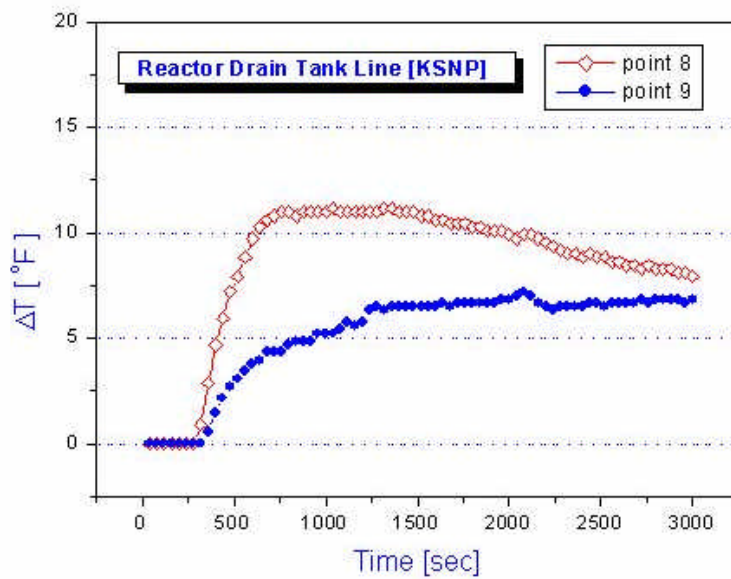


Fig. 12 The temperature difference changes between top and bottom inner wall at the point 8 and 9 for the variations of time

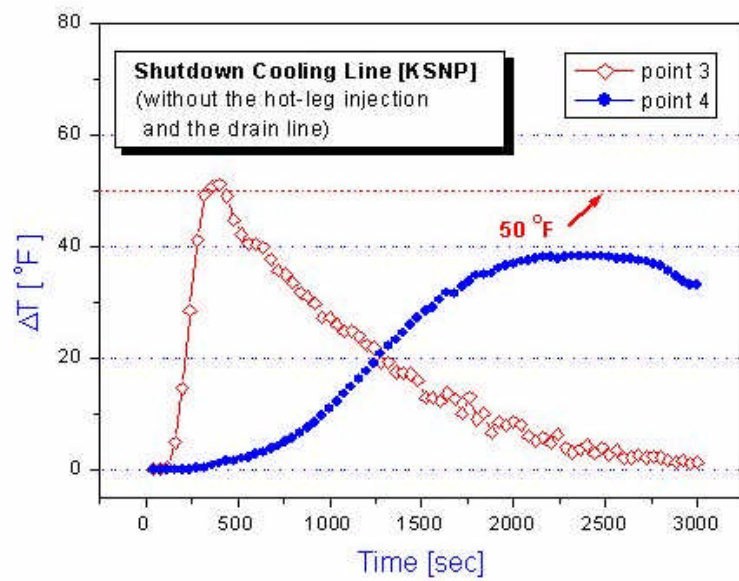


Fig. 13 The temperature difference changes between top and bottom inner wall at the point 3 and 4 for the variations of time (the case that the hot-leg injection piping and drain piping are not connected with the SCS piping)